



APPLICATION OF THE RESISTIVITY METHOD IN THE KRÍSUVÍK GEOHERMAL AREA, REYKJANES PENINSULA, SW-ICELAND

Yiheyis Kebede

Geological Survey of Ethiopia,
Hydrogeology, Engineering Geology and Geothermal Studies Department,
P.O. Box. 27845, Addis Ababa,
ETHIOPIA
geology@telecom.net.et

ABSTRACT

This report describes resistivity measurements made in the Krísuvík geothermal area, Reykjanes Peninsula, SW-Iceland. The report includes the theoretical aspects of the resistivity methods in geothermal exploration and interpretation and comparison of sounding results, based on DC methods (Schlumberger configuration) and EM methods (Central-loop transient electromagnetic - TEM) are made and presented.

The resistivity structure of the Krísuvík geothermal area is observed to reveal several resistivity layers, including high resistivity ($\geq 200 \Omega\text{m}$) near the surface that is related to cold and fresh basaltic rock of Postglacial volcanism, moderately high resistivity (50-200 Ωm) related to slightly altered rocks due to groundwater action, moderate resistivity (10-50 Ωm) related to moderately hydrothermally altered rocks, and low resistivity ($\leq 10 \Omega\text{m}$) related to low-temperature (50-200°C) alterations in the smectite-zeolite zone. The typical resistivity structure that is observed in most high-temperature geothermal fields of Iceland (e.g. Krafla and Nesjavellir), with high resistivity below a low-resistivity cap rock, is also seen in the Krísuvík geothermal area. This resistivity structure is interpreted as a result of the chlorite alteration zone that is of temperatures higher than 240°C.

Comparisons of results of the two methods show that a similar resistivity structure could be obtained using both methods but with slight discrepancies that arise basically from their principles and methodology. Experience in resistivity mapping of geothermal fields of Iceland and this study indicate that the resistivity structure of geothermal prospects is best mapped using the TEM method, especially in areas with dry and highly resistive surface conditions, like volcanic lava, combined with low-resistivity formations at deeper levels, which is common for geothermal fields.

1. INTRODUCTION

Geophysics is a science that serves in the investigation of the earth by making use of measurements of the physical parameters associated with earth materials (rocks, minerals, water, etc.). The physical parameters

include electrical resistivity or conductivity, magnetic susceptibility, density, radioactivity, thermal conductivity, elasticity, sound velocity, etc. The response of the earth solely depends on the natural variation of the physical parameters mentioned.

Geophysical methods have a significant role in the investigation of geothermal prospects because they are the only means to find deep sub-surface structures at a much lower cost than the most direct method, drilling. A relatively large area can be investigated within a short time using geophysical methods. Methods in geophysical exploration are classified as *active* and *passive* methods based on the nature of the stimulus used in the measurements. An active method makes use of an artificially created or applied field (external field of controlled source) and measures the response of the earth using a receiver. In geothermal studies, such methods include DC resistivity, transient electro-magnetic and seismic methods and they are used in determining the parameters directly related with geothermal reservoirs. A passive method makes use of measurements of natural field variations in order to investigate the parameter to be studied. Examples of such methods are gravity, magnetic, micro-seismicity, etc. (referred to as structural methods in geothermal exploration), and they serve in a regional reconnaissance surveys to locate geological structures, calderas, dykes, concealed plutonic bodies, faults etc., that could be related to the geothermal resources.

In geothermal exploration the choice of a particular method depends on the objective and the cost of the survey. It should be noted that there is no single method or combination of different methods that can be called optimum in all cases. The most suitable method may vary for different geothermal fields. In Iceland, the thermal method, electrical resistivity, and transient electro-magnetic (TEM) methods, and passive seismicity stand out among the others in the study of geothermal reservoirs.

The application of geophysical methods for geothermal exploration in Iceland dates back 50 years. The most widely used method was the DC resistivity method using the Schlumberger configuration. The method was used until 1986 in regional resistivity mapping of the Icelandic crust and for mapping of vertical resistivity structures both within and outside the volcanic zone. Starting from 1986, the central-loop TEM method has become popular and soon succeeded the Schlumberger method as the main tool in the mapping of resistivity structures of the geothermal fields in Iceland (Árnason, 1989).

The present work is the final part of the geothermal training that the author underwent during April to October 2001 at the United Nations University (UNU) Geothermal Training Programme, at Orkustofnun - the National Energy Authority in Iceland. The aim of the training was to give a practical knowledge of the application of geophysical methods in geothermal fields. Special emphasis was put on the resistivity methods using Schlumberger and central-loop transient electromagnetic (TEM) soundings so that a good understanding of the methods, data processing, and interpretation using a one-dimensional model could be obtained. The project is based on Schlumberger data collected in the eighties and TEM data collected later on in the Krísuvík area (sometimes written as Krýsuvík area), Reykjanes Peninsula. The field survey was carried out by geophysicists from Orkustofnun.

2. RESISTIVITY OF ROCKS

First we concentrate on the definition and units of resistivity measurements, but then on factors affecting resistivity, ρ of geothermal reservoir rocks.

2.1 Definition and unit of resistivity

The electrical resistance refers to the resistance of a body to a flow of electric current through it. The electrical resistance, R , of the sample shown in Figure 1 is proportional to its length L and inversely proportional to its cross-sectional area A , and is given by:

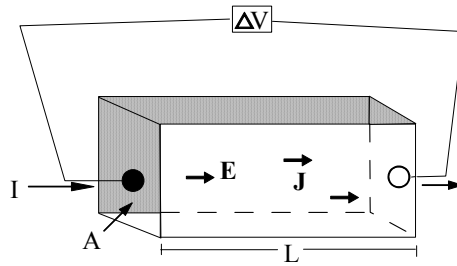


FIGURE 1: A sample of a material having a cross-sectional area A and length L

$$R \propto L / A \quad \text{or} \quad R = \rho L / A \quad (1)$$

where R = Electrical resistance [Ω];
 ρ = Proportionality constant, called electrical resistivity [Ωm];
 L = Length of the body [m];
 A = Cross-sectional area of the body [m^2].

According to Ohm's law, the resistance of a wire or similar is given by:

$$R = \Delta V / I \quad (2)$$

where ΔV = Potential difference across the sample [V];
 I = Electric current through the sample [A].

By substituting Equation 1 into 2, we obtain the formula for calculating the resistivity as:

$$\rho = \frac{A \Delta V}{L I} \quad (3)$$

The above equation may be used to determine the resistivity of a homogeneous and isotropic material (regular geometric shape, cylinder, parallelepiped, and cubes). In a semi-infinite material the resistivity at every point must be defined. If the cross-sectional areas and length of an element within the semi-infinite material are shrunk to infinitesimal size, then the resistivity ρ may be defined as (Zohdy et al., 1980):

$$\begin{aligned} & \lim (\Delta V / L) \\ & = \frac{\lim_{L \rightarrow 0} (\Delta V / L)}{\lim_{A \rightarrow 0} (I / A)} \quad \text{or} \quad \rho = \frac{\bar{E}}{\bar{J}}, \quad \bar{J} = \sigma \bar{E} \end{aligned} \quad (4)$$

where \bar{E} = Electric field [V/m];
 \bar{J} = Current density [A/m^2];
 σ = Conductivity [S].

The electrical resistivity, ρ , or the specific electrical resistance of a material is an inherent characteristic of the material or the sample and is independent of the shape and size of the sample.

2.2 Factors affecting resistivity of rocks and minerals

The resistivity of rocks varies from 10^{-8} - 10^{-7} Ωm for pure metals such as gold, to 10^{10} - 10^{12} Ωm for non-conducting substances such as quartz. It should be noted that every rock type, mineral and ore has a range of resistivities, depending on different factors. The resistivity range of typical Icelandic rocks is described in Table 1 below (Björnsson, 1980).

TABLE 1: Typical resistivity values of Icelandic rocks

Rock type	Resistivity (Ωm)
Recent lava flows, above groundwater level	5,000 - 50,000
Dense intrusive (gabbros, dolerite)	10,000 - 15,000
Recent lava flows, below groundwater level	100 - 3,000
Basalts, rather dense	100 - 300
Low-temperature areas in basalt formations	30 - 100
High-temperature areas in chlorire-epidote zone, fresh water	20 - 100
Cold rocks with brine	5 - 15
High-temperature areas, in smectite-zeolite zone, fresh water	1 - 10
High-temperature areas, brine areas	1 - 4

The electrical resistivity of rocks depends on the following factors:

- Porosity and the pore structure of the rocks;
- Amount of water (saturation);
- Salinity of the water;
- Temperature;
- Pressure;
- Water-rock interaction and alteration;
- Steam content in the water.

Electrical conductivity in minerals and solutions takes place by the movement of electrons and ions. In rocks, the conduction of electricity is in most cases through water contained in the pores of the rocks and along the interface layer of the rocks and solution.

2.2.1 Archie's law

One of the main factors that affects resistivity of geothermal reservoir rocks, and resistivity of water-saturated rocks in general, is porosity. There is an empirical relationship called Archie's law that describes this (Archie, 1942). It describes how the resistivity depends on porosity if ionic conduction in the pore fluid dominates other conduction mechanisms in rocks. Archie's law is given by the equation

$$\rho = \rho_w a \phi_t^{-n} \quad (5)$$

where ρ = Bulk (measured) resistivity;
 ρ_w = Resistivity of pore fluid;
 Φ_t = Porosity in proportion to total volume;
 a = An empirical parameter; varies from less than 1 for intergranular porosity to over 1 for joint porosity, but it is usually around 1;
 n = Cementing factor, an empirical parameter; varies from 1.2 for unconsolidated sediments to 3.5 for crystalline rocks, but is usually around 2.

Archie's law can be written as a ratio of the bulk resistivity to the resistivity of the pore fluid, called formation factor, F . The formation factor is constant for a given porosity and is written as

$$F = \frac{\rho}{\rho_w} = a \cdot \phi^{-n} \quad (6)$$

Archie's law is valid for Icelandic rocks if the resistivity of the pore fluid is of the order of 2 Ωm or less, but doubts arise if the resistivity is much higher (Flóvenz et al., 1985). The law relates the effective resistivity of a rock to the porosity of the rock, the fraction of the pores filled by the pore fluids (degree of saturation), and the resistivity of the pore fluids.

2.2.2 Effect of chemical concentration and temperature

In aqueous salt-solution the mobility of ions depends on concentration and temperature of the solution (Hersir and Björnsson, 1991). The conductivity $\sigma(1/\rho)$ of a solution may be written as

$$\sigma = 1/\rho = F \cdot (c_1 q_1 m_1 + c_2 q_2 m_2 + \dots) \quad (7)$$

where F = Faraday's number (96,500);
 c_i = Concentration of ions;
 q_i = Valence of ions;
 m_i = Mobility of different ions.

Experimental results show in accordance with the above equation that the resistivity is nearly inversely proportional to the salinity of electrolytes, such as NaCl in water (Keller and Frischknecht, 1966). For $T = 0$ the following relationship is observed:

$$\rho = 9.545 C^{-0.937} \approx \frac{10}{C} \quad (8)$$

where C = Concentration of NaCl [g/l].

At moderate temperatures, 0-200°C, the resistivity of aqueous solutions decreases with increasing temperature. Temperature affects the mobility of the ions because the increased temperature reduces the viscosity of the water and hence increases the mobility of the ions. Dakhnov, (1962) has described this relationship as:

$$\rho_w = \frac{\rho_{w_0}}{1 + \alpha(T - T_0)} \quad (9)$$

where ρ_{w_0} = Resistivity of the fluid at temperature T_0 ;
 α = Temperature coeff. of resistivity, $\approx 0.023^\circ\text{C}^{-1}$ for $T_0 = 23^\circ\text{C}$ and 0.025°C^{-1} for $T_0 = 0^\circ\text{C}$.

At high temperatures, a decrease in the dielectric permittivity of the water results in a decrease in the number of dissociated ions in solution. Above 300°C, this starts to increase fluid resistivity (Quist and Marshall, 1968).

2.2.3 Effect of water-rock interaction

The resistivity of rocks decreases due to conduction along the interface between rock and water. This relationship is expressed as:

$$\sigma = \frac{1}{F} \sigma_w + \sigma_s \quad (10)$$

where σ = Total conductivity;
 σ_w = Conductivity of the pore water;
 σ_s = Interface conductivity;
 F = Formation factor.

Several relationships have been developed where interface conductivity dominates both matrix and pore fluid conduction. Flóvenz, et al., (1985) established the following equation relating the bulk resistivity ρ , to the fracture porosity ϕ_f , the temperature T and the pore fluid resistivity ρ_{w0} , at $T_0 = 23^\circ\text{C}$.

$$\frac{1}{\rho} = \frac{0.22}{\rho_w} \left[1 - (1 - \phi_f)^{2/3} + \frac{(1 - \phi_f)^{2/3}}{1 + (1 - \phi_f)^{1/3} + (1 - \phi_f)^{1/3} 4.9 \cdot 10^{-3}} \right] + \frac{\phi_f^{1.06}}{b} \quad (11)$$

where

$$\rho_w = \rho_{w0} / [1 + 0.023(T - 23)] \quad \text{and} \quad b = 8.7 / [1 + 0.023(T - 23)] [1 + 0.018(T - 23)]$$

This equation has been found applicable for the uppermost kilometre of the Icelandic basaltic crust for the temperature of up to at least 100°C . In Equation 11 the last expression in the right hand side is the same as the surface conduction σ_s in Equation 10, whereas the other expressions represents pore fluid conduction according to the double-porosity model put forward by Stefánsson et al. (1982).

2.3 Resistivity structure of high-temperature geothermal systems in the basaltic crust of Iceland

Equation 11 holds for low-temperature geothermal fields outside the volcanic zone. Resistivity surveys in the high-temperature geothermal systems within the basaltic crust of Iceland all reveal a similar resistivity structure, characterized by a low-resistivity cap at the outer margins of the reservoir underlain by a more resistive core towards the inner part, as observed by Árnason et al. (2000). Comparison of well data with this structure shows a good correlation between the resistivity structure and alteration mineralogy. The low resistivity in the cap rock is dominated by conductive minerals in the smectite-zeolite zone at temperatures of $100\text{-}200^\circ\text{C}$. In the temperature range of $200\text{-}240^\circ\text{C}$ zeolites disappear and smectite is gradually replaced by resistive chlorite. At temperatures exceeding 250°C chlorite and epidote are the dominant minerals and the resistivity is probably dominated by the pore fluid conduction in the high-resistivity core. The situation is the same in the geothermal systems with fresh and saline water but values of resistivities are much lower in the saline systems. A similar resistivity structure is to be expected in acidic rocks but due to different alteration mineralogy the transition from the conductive cap to the more resistive core occurs at temperatures lower than 200°C .

3. THEORETICAL BACKGROUND OF DC RESISTIVITY MEASUREMENTS

In the DC resistivity methods the resistivity of the rocks is measured by transmitting constant current in to the ground and measuring the response, the potential between two points, using a special measuring device, the receiver. The theoretical aspect of the method is discussed in the following sections. This section deals with the theoretical background for the resistivity survey and the derivation of the relationship for the apparent resistivity of the Schlumberger soundings. Finally, the theory of one-dimensional interpretation over a horizontally stratified earth will be discussed.

3.1 Point source on homogeneous earth

The potential distribution due to a single current source at the surface of a homogeneous earth is a function of distance r from the source as shown in the Figure 2.

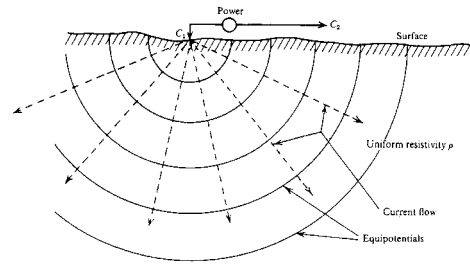


FIGURE 2: Current and potential distribution due to a single current source

The current density, at any point at a distance r away from the source is given by $j = I/2\pi r^2$ where I is the injected current. The current i through a differential element ds is $i = j ds$, and the resistance of the element, dv , is $R = \rho dr/ds$.

Ohm's law, Equation 2, in a differential form can be written as

$$dV = -R j$$

Substituting the expressions for j and R into the formula for the potential dV and integrating the result gives,

$$V(r) = - \int \frac{\rho I}{2\pi r^2} dr + C = \frac{\rho I}{2\pi r} + C$$

The potential is set to zero at infinity, $V(\infty) = 0$, so that $C = 0$ and we obtain the expression for the potential generated by a single point source of current I , at the surface of an electrically homogeneous earth to be a function of the radial distance from the source point (Koefoed, 1979):

$$V(r) = \frac{\rho I}{2\pi r} \tag{12}$$

It should be noted that for a more realistic case, the case of two current electrodes, the algebraic sum of the result obtained for a single electrode could be utilized.

3.2 Horizontally layered earth

The derivation of the potential due to a point source over a horizontally layered half-space, as shown in Figure 3, is made by making the following assumptions (Koefoed, 1979, after Stefannescu et al., 1930):

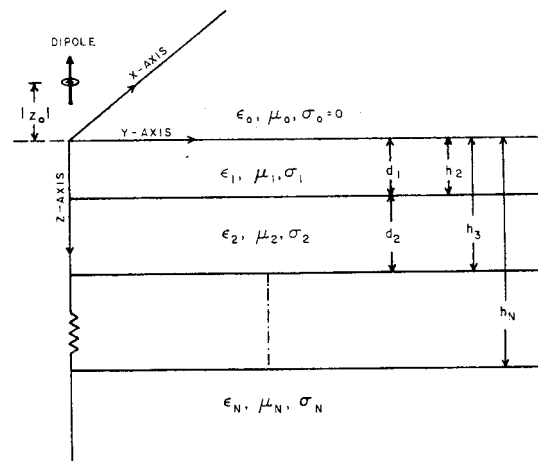


FIGURE 3: Diagram showing the parameters of an n layered strata

- The subsurface consists of a finite number of layers with finite thickness and the deepest layer extended to infinity; the layers are separated from each other by horizontal boundary planes;
- Each of the layers is electrically homogeneous as well as electrically isotropic;
- The field is generated by a current source that is located at the surface of the earth;
- The current emitted by the source is direct current.

From the potential field theory the electric field \vec{E} , is the negative gradient of the potential V and is written as

$$\vec{E} = -\vec{\nabla} V \quad (13)$$

Taking the divergence of Equation 4, the relationship of the electric field and the current density can be written as

$$\vec{\nabla} \cdot \vec{J} = \vec{\nabla} \cdot \sigma \vec{E} \quad (14)$$

Using the second assumption, i.e. the medium to be electrically homogeneous (σ constant), and substituting Equation 13 into Equation 14, the following relation is valid in each layer

$$\vec{\nabla} \cdot \vec{J} = \vec{\nabla} \cdot \sigma_i \vec{E} = -\sigma_i \nabla^2 V \quad (15)$$

From the third assumption, the divergence of the current density \vec{J} , is zero except at the surface of the upper most layer hence the above equation has a form,

$$\vec{\nabla} \cdot \vec{J} = I \delta(\vec{X}) \quad (16)$$

where $\delta(\vec{X})$ is called Dirac delta function. Its value is equal to zero for all \vec{X} except at the point of the current source. By equating Equations 15 and 16 and using the relationship $\sigma = 1/\rho$, and taking $\rho = \rho_1$, i.e. the resistivity of the first layer, the following relationship is obtained,

$$-\nabla^2 V = \rho_1 I \delta(\vec{X}) \quad (17)$$

Equation 17 is an inhomogeneous differential equation of the second order and has a special solution given by Equation 12 in the previous section (Árnason and Hersir, 1988)

$$V = \rho_1 I / 2\pi R \quad (18)$$

where $R = (x^2 + y^2 + z^2)$

Transforming this equation into cylindrical coordinates, Equation 18 can be written as

$$V = \frac{\rho_1 I}{2\pi} (r^2 + z^2)^{-1/2} \quad (19)$$

Using an integral from the theory of Bessel's functions known as the Lipschitz integral

$$\frac{1}{\sqrt{r^2 + z^2}} = \int_0^{\infty} e^{-\lambda z} J_0(\lambda r) d\lambda$$

where $J_0(\lambda r)$ is Bessel's function of zero order, Equation 19 can be written as

$$V = \frac{\rho_1 I}{2\pi} \int_0^{\infty} e^{-\lambda z} J_0(\lambda r) d\lambda \quad (20)$$

the solution for the uppermost layer. For the other layers $i > 1$ (i.e. in the source free media), the Dirac delta function $\delta(\vec{X}) = 0$, and Equation 17 is reduced to

$$\nabla^2 V = 0 \quad (21)$$

This equation is known as Laplace's equation. In a Cartesian coordinate system it is written as

$$\nabla^2 V = \frac{\partial^2 V}{\partial^2 x} + \frac{\partial^2 V}{\partial^2 y} + \frac{\partial^2 V}{\partial^2 z} \quad (22)$$

In a homogeneous and isotropic media the potential distribution is uniform and symmetrical about the z axis through the source and is independent of the angle θ . Hence, Equation 22 in cylindrical coordinates becomes

$$\frac{\partial^2 V}{\partial^2 r} + \frac{1}{r} \frac{\partial V}{\partial r} + \frac{\partial^2 V}{\partial^2 z} = 0 \quad (23)$$

The solution to Equation 23 is obtained by the method of separation of variables resulting in two second-order ordinary differential equations. Any linear combination of the product of the solutions of these differential equations is also a solution to Equation 23 (see Koefoed, 1979, pages 21-22). Hence for the i -th layer it can be written as

$$V_i = \frac{\rho_1 I}{2\pi} \int_0^\infty [e^{-\lambda z} + \Theta_i(\lambda)e^{-\lambda z} + X_i(\lambda)e^{+\lambda z}] J_0(\lambda r) d\lambda \quad (24)$$

where $\Theta_i(\lambda)$ and $X_i(\lambda)$ are functions of λ .

The following boundary conditions are used to determine the functions Θ and X :

1. At each of the boundary planes in the subsurface the electrical potential must be continuous, i.e. $V_i(h_i) = V_{i+1}(h_i)$;
2. At each of the boundary planes in the subsurface, $\frac{1}{\rho_i} \frac{\partial V_i}{\partial z} = \frac{1}{\rho_{i+1}} \frac{\partial V_{i+1}}{\partial z}$ at $z = h_i$;
3. At the surface plane the vertical component of the current density, and hence that of the electrical field intensity, must be zero everywhere except in an infinitesimal neighbourhood around the current source, ($J_z = 0$ and $E_z = 0$);
4. Near the current source the potential must approach infinity and at infinite depth the potential must approximate zero.

The evaluation of Equation 24 using the boundary conditions is discussed in Koefoed, (1979, pages 23-25) and, as a result, the general solution to the inhomogeneous Equation 17 at the surface is found to be

$$V = \frac{\rho_1 I}{2\pi} \int_0^\infty [1 + 2\Theta_1(\lambda)] J_0(\lambda r) d\lambda \quad (25)$$

In order to evaluate the integral Equation 25, the so-called digital filter method is used. The expression in the parenthesis of the above integral is expressed as

$$K(\lambda) = 1 + 2\Theta_1(\lambda) \quad (26)$$

Both the functions $K(\lambda)$ and $\Theta_1(\lambda)$ are referred to as kernel functions and are controlled by the resistivities of the layers, ρ_i , and by depths of the boundary planes, h_i .

Applying the boundary conditions to Equation 24 and making arrangements of the results leads to the following expression

$$\rho_i \frac{1 + \Theta_i(\lambda) + X_i(\lambda)e^{+2h_i}}{1 + \Theta_i(\lambda) - X_i(\lambda)e^{+2h_i}} = \rho_{i+1} \frac{1 + \Theta_{i+1}(\lambda) + X_{i+1}(\lambda)e^{+2h_i}}{1 + \Theta_{i+1}(\lambda) - X_{i+1}(\lambda)e^{+2h_i}} \quad (27)$$

and defining

$$K_i = \frac{1 + \Theta_i(\lambda) + X_i(\lambda)e^{+2h_i}}{1 + \Theta_i(\lambda) - X_i(\lambda)e^{+2h_i}} \quad (28)$$

In the first layer where $h_{i-1} = 0$, and $\Theta_i(\lambda)$ and $X_i(\lambda)$ the expression will become

$$K_1(\lambda) = 1 + 2\Theta_1(\lambda) \quad (29)$$

Mathematical manipulation on Equation 27 and making use of the relationship for hyperbolic tangent function

$$(e^{2\lambda t_i} - 1)/(e^{2\lambda t_i} + 1) = \tanh(\lambda t_i)$$

the following relationship is obtained

$$K_i = \frac{K_{i+1} + p_i \tanh(\lambda t_i)}{p_i + K_{i+1} \tanh(\lambda t_i)} \quad (30)$$

where $t_i = h_i - h_{i-1}$, is the thickness of the layer and $p_i = \rho_i/\rho_{i+1}$. The definition of K together with boundary condition (5) will result for the basement (the n^{th} layer) $K_n = 1$. Starting with this expression in the basement, the K function in the layers above can be determined by recurrent application of Equation 30.

3.3 The Schlumberger sounding method

3.3.1 Apparent resistivity and the gradient approach

In the Schlumberger configuration the current transmitting and the signal receiving potential electrodes are placed symmetrically along a straight line as shown in Figure 4, the current electrodes on the outside and the potential electrodes on the inside. The depth of penetration is increased by increasing the current electrode spacing $AB/2$ while the spacing between the potential probes is kept constant at the centre until the potential detected becomes weaker. The result of the survey is presented as a vertical electrical sounding curve (VES curve) to show the depthwise variation of the resistivity structure of the crust or as a plan map or profile curves to show the aerial subsurface resistivity distribution at a fixed depth level.

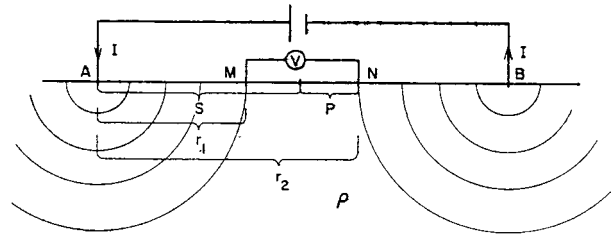


FIGURE 4: Electrode configuration of the Schlumberger survey

In the Schlumberger configuration the potential difference, ΔV between the two measuring points M and N due to the current sources at A and B on homogeneous earth with resistivity ρ , can be derived using the formula obtained for a single current electrode source as

$$\Delta V = V_M - V_N = \frac{\rho I}{2\pi} \left(\frac{1}{r_1} - \frac{1}{r_2} \right) = \frac{\rho I}{K}$$

or

$$\rho = \frac{\Delta V}{I} K \quad (31)$$

where K is a geometric factor and is defined by

$$K = \pi \frac{1}{\frac{1}{r_1} - \frac{1}{r_2}} \quad (32)$$

Using $r_1 = S-P$, $r_2 = S+P$, Equation 32 becomes

$$K = \pi \frac{S^2 - P^2}{2P} \quad (33)$$

where $S = AO = OB$, $P = MO = NO$

Substituting this into Equation 31 the expression for resistivity using the finite electrode spacing becomes,

$$\rho = \frac{\pi}{2} \frac{S^2 - P^2}{P} \frac{\Delta V}{I}$$

In reality the subsurface is inhomogeneous and hence the value obtained is not the true resistivity but the so called apparent resistivity, ρ_a , hence the above equation becomes,

$$\rho_a = \frac{\pi}{2} \frac{S^2 - P^2}{P} \frac{\Delta V}{I} \quad (34)$$

This equation relates the subsurface apparent resistivity distribution to the surface measurement.

In the interpretation of the Schlumberger sounding, it is often assumed that the distance between the potential electrodes to be infinitesimal, i.e. $P \ll S$, and it is called the gradient approach.

The potential difference ΔV between M and N can be written as,

$$\Delta V = V_M - V_N = [V(S-P) - V(S+P)] - [V(S+P) - V(S-P)] = 2[V(S-P) - V(S+P)] \quad (35)$$

Hence,

$$\rho_a = \frac{2\pi}{I} \frac{[V(S-P) - V(S+P)]}{2P} (S^2 - P^2) \quad (36)$$

If $P \ll S$, this can be approximated as

$$\rho_a = -\frac{2\pi}{I} \frac{dV}{dr} \Big|_{r=S} \cdot S^2 \quad (37)$$

After mathematical manipulation on the general solution of the differential Equation 17, an expression for the potential at the surface of layered earth is found to be (Koefoed, 1979),

$$V = \frac{\rho_{1l}}{2\pi} \int_0^\infty [1 + 2\Theta_1(\lambda)] J_0(\lambda r) d\lambda$$

Then by using the property of Bessel's functions,

$$\frac{\partial}{\partial r} J_0(\lambda r) = -\lambda J_1(\lambda r)$$

a formula for the apparent resistivity is obtained that is readily evaluated using the digital filter,

$$\rho_a = \rho_1 + 2\rho_1 S^2 \int_0^{\infty} \Theta_1(\lambda) J_1(\lambda S) \lambda d\lambda \quad (38)$$

where J_1 is Bessel's function of first order.

3.3.2 Factors affecting Schlumberger sounding curves

There are several factors that affect results of the resistivity measurements. In a Schlumberger survey, erroneous data are mostly fixed at the field site. The most common conditions that affect the resistivity curves are near-surface inhomogeneities, topography, and inhomogeneities and anisotropy.

Near-surface inhomogeneities. In Schlumberger sounding the signal received by the receiver decreases as the current electrode spacing, S increases. In order to obtain a measurable signal at the centre it is required to increase the potential spacing, P . The effect of this increment in the potential electrode spacing can be reflected on the apparent resistivity curve as a shift on a log-log plot. There are two types of shifts. The first is called converging shift and is due to the variation of resistivity with depth. The second type of shifts is called constant shift and is caused by inhomogeneities close to the potential electrodes, which leads the interpretation astray (Árnason, 1984). The way to handle these shifts is to fix the segment of the curve measured with the largest P , used in the sounding and correct the others by a factor that forces the segments to tie in. The depth of penetration of Schlumberger sounding is not only a function of the distance between the current electrodes $2S$. It is actually a function of the shortest distance between the current and potential electrodes ($S - P$) (Árnason, 1984). For the same S and different P , different values of ρ_a reflect different resistivity at different depths. For instance, if the difference ($S - P$) in a two-layer case is of the same order of magnitude as the depth to the layer boundary, the measured ρ_a value will be dominated by the resistivity of the first layer, independent of the distance between the current electrodes.

One of the effects of inhomogeneities is the phenomenon known as equivalence and suppression. Strongly differing layer distribution in the subsurface may yield apparent resistivity curves that, although not strictly equal, differ so slightly, that they cannot be distinguished within the accuracy of measurements (Koefoed, 1979). The phenomena can either be 'an equivalence' or 'suppression'. There are two types of equivalence. In both cases the depth to this layer's interface, must be the same or less than the thickness of the undetermined layer. The first one is a bell type curve, i.e. a resistive layer that is embedded between two conductive layers. In this case the only known parameter for the intermediate layer, is the transversal resistance, given by the product $p_i d_i = T_i$. The second one is a bowl type curve, i.e. a conductive layer that is embedded between two resistive layers. In this case, the only known parameter for the intermediate layer is the longitudinal conductance, given by the quotient $d_i / \rho_i = S_L$. Suppression may occur in monotonically increasing or decreasing types of resistivity variations. In this case the existence of an intermediate layer may not be detected from the resistivity curve. In the one-dimensional interpretation it is advisable to add some independent information from other investigations or correlations with other neighbouring sounding curves should be made.

Topography. The flow of current is affected by topographic variation, which in turn affects the nature of the equi-potential surfaces. This results in distortion of the potential distribution in such a way that current density i is concentrated in topographic lows (valleys) but reduced in topographic highs (ridges). Hence, the measured potential difference and apparent resistivity increases in valleys, but decreases on ridges.

Inhomogeneities and anisotropy. The assumptions made in Section 3.2 are not encountered quite often in nature. In reality geological formations may be electrically anisotropic, that is the conductivity σ , dielectric permittivity ϵ , and magnetic permeability μ may depend on direction. It should be noted that in the derivation of the Laplace equation, the assumptions made are valid if the resistivity variations within the layers are not exaggerated. The phenomena are quite common in formations rich in clay or shale. In

these conditions the electrical resistivity is the same in all directions along a layer but have values higher in the direction perpendicular to the stratification.

3.3.3 One-dimensional interpretation

The computer program used in the processing and interpretation of the data are PSLINV and SLINV. The programs are operated in any PC that supports FORTRAN77. The field data are manually entered into the PC using PSLINV. The program averages repeated measurements, calculates apparent resistivities and determines shift factors needed to correct for shifts between overlapping segments measured by different potential electrode spacings. It outputs apparent resistivity curves for monotonically increasing $AB/2$ values ready for an inversion program, SLINV (Schlumberger INVersion). SLINV is a non-linear least-square inversion program using the Levenberg Marquardt algorithm together with a fast forward routine based on the digital filter method (Árnason and Hersir, 1988). The inversion program reads the measured apparent resistivity from an input file. The operator gives an initial guess model and the program iteratively adjusts the layer resistivities and thicknesses until the difference between the measured and calculated apparent resistivity values are minimum. The output plot file and list file are products of the program.

The program does not adjust the number of layers, and several models with different numbers of layers are fitted to the measured curve. Normally the model that fits the curve satisfactorily with fewer layers is taken as the best model.

4. TRANSIENT ELECTROMAGNETIC SOUNDING

4.1 Scope of the method

The Transient Electro Magnetic (TEM) method is one of the active geophysical methods used in the exploration of geothermal resources in Iceland. In the volcanic zones where the surface is mostly covered by lava, current injection into the ground is a major problem when using Schlumberger soundings. In the TEM method no current is injected to the ground, but into a source loop at the surface. In addition to this, the method has a couple of advantages over the conventional Schlumberger DC-sounding. The popularity of the method is increasing and now it serves as one of the best tools in geothermal exploration, especially in areas with highly resistive ground conditions. The method has been widely used in geothermal exploration of Iceland since 1986.

4.2 Theoretical background of the TEM method

The electromagnetic (EM) method is classified as frequency domain or time domain, depending on the measuring techniques employed. The time domain electromagnetic methods (TEM) are further classified as grounded-dipole or loop source methods depending on how the source field is introduced into the ground. In the central-loop method (Figure 5), a

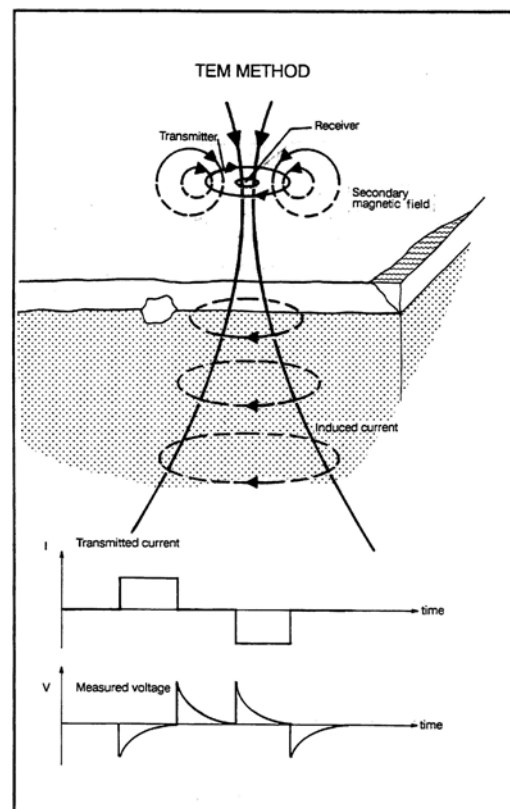


FIGURE 5: The central-loop TEM sounding configuration (Hersir and Björnsson, 1991)

loop of wire is placed on the ground and a constant magnetic field of known strength is built up by transmitting a constant current into the loop. The current is abruptly turned off. The decaying magnetic field induces electrical current in the ground.

The current distribution in the ground induces a secondary magnetic field decaying with time. The decay rate of this magnetic field is monitored by measuring the voltage induced in a receiver coil (or small loop) at the centre of the transmitter loop, as shown in Figure 5. The current distribution and the decay rate of the secondary magnetic field depend on the subsurface resistivity structure.

The depth of penetration in the central loop TEM-sounding is dependent on how long the induction in the receiver coil can be traced before it is drowned in noise. At late times, the induced voltage in the receiving coil on a homogeneous half space of conductivity, σ is approximately given by (Árnason, 1989)

$$V(t, r) = I_0 \frac{C (\mu_0 \sigma r^2)^{3/2}}{10 \pi^{1/2} t^{5/2}} \quad (39)$$

where $C = A_r n_r A_s n_s \frac{\mu_0}{2\pi r^3}$

- and
- A_r = Cross-sectional area of the receiver coil [m²];
 - n_r = Number of turns on the receiver coil;
 - A_s = Area of the transmitting loop [m²];
 - n_s = Number of turns in transmitter loop;
 - t_r = Time elapsed after the current in the transmitter is turned off [s];
 - μ_0 = Magnetic permeability [Henry/m];
 - $V(t, r)$ = Transient voltage[V];
 - r = Radius of the transmitter loop [m];
 - I_0 = Current in the transmitting loop [A].

Substituting $\sigma = 1/\rho$ in Equation 39 and solving for the resistivity, the following relationship is obtained:

$$\rho_a = \frac{\mu_0}{4\pi} \left[\frac{2I_0 A_r n_r A_s n_s}{5t^{5/2} V(t, r)} \right]^{2/3} \quad (40)$$

This relationship defines a late time apparent resistivity.

4.3 Instrumentation, data processing and presentation of TEM data

The instrument used to collect the central-loop TEM data discussed in this report, the Protem/EM 37 from Geonics Ltd., consists of a current transmitter, generator, receiver box, receiver and transmitter loops. A small coil with an effective area of 100 m², and a flexible loop with an effective area of 5000 m² were used as receiver antennas and a square transmitter loop of 300 m side length. The transmitted current is usually in the range of 20-24 A, and the transient signal is recorded in the time interval of 0.087-70.4 ms at 30 logarithmically spaced channels after the current turn-off. Both the transmitter and receiver timing are controlled by synchronized high precession crystal clocks. The induced voltage is measured by the receiver each time the transmitter is turned off. Data were recorded for two transmitter frequencies. At high frequency the repetition rate of the transmitted current signal is 25 Hz, with 10 ms current off segments. At low frequency the repetition rate is 2.5 Hz, with current off segments of 100 ms. Then the data are edited to remove electromagnetic noise to obtain induced voltage and finally, apparent resistivity is calculated as a function of time.

4.4 One-dimensional interpretation

Two computer programs TEMPREP and TINV (TEM-INVersion) were used in the processing and interpretation of the central-loop TEM data. The programs run on any PC that supports FORTRAN77 (Árnason, 1989). The raw data are dumped from the receiver and edited (removal of electromagnetic noise) using the program TEMPREP. The program TINV was used for one-dimensional inversion of TEM soundings. The program assumes that the field data is collected with equipment where the transmitted current is turned off linearly from maximum to zero and that the time values, at which the apparent resistivity values are given, are equally spaced in logarithm of time after the current has become zero. This program assumes that data are collected with a circular loop. If this is not the case the actual transmitter loop is simulated by a circular loop having the same area.

5. RESISTIVITY SURVEY IN THE KRÍSUVÍK AREA

5.1 Regional geology and geological settings of the study area

The constructive plate boundaries between the North-American and Eurasian plates follow the Mid-Atlantic Ridge and cross Iceland from southwest to northeast. In Iceland, rifting, spreading, and volcanic activity characterize the boundaries. The crust formed in the volcanic rift zone is composed of basaltic lavas with some acidic and intermediate rocks in volcanic centres. Extension and subsidence in the rift zone is matched by intrusions and subaerial lava flows resulting in a lava pile tilting gently ($5\text{--}10^\circ$) toward the volcanic zone. Owing to the crustal spreading, the lava pile is moved away from the zone of accretion, hence the age of the crust increases away from the volcanic zone. Based on climatic evidence from inter-lava sediments or volcanic breccias and/or paleomagnetic reversal patterns supported by absolute age data, the volcanic pile of Iceland is conventionally divided into four stratigraphic groups or series (Saemundsson, 1979). The four groups are Postglacial (9000-13000 years), Upper Pleistocene (back to 0.7 m.y.), Plio-Pleistocene (0.7-3.1 m.y.), and Tertiary rocks (older than 3.1 m.y.).

The magmatic activity and volcanism result in high heat flow in the Icelandic crust. And the mean heat flow decreases with increasing distance from the volcanic rift zone. Geothermal fields in Iceland are classified into two categories (Fridleifsson, 1979). High-temperature fields (confined to the active zones of rifting and volcanism) have temperatures higher than 200°C in the uppermost one km, and low-temperature fields (mostly found outside the active zone within the Quaternary and Tertiary rock units) with temperatures lower than 200°C above 1 km depth.

The Krísuvík area (Krýsuvík area) is located on the Reykjanes Peninsula within the active zone of rifting and volcanism (Figure 6). It is a high-temperature geothermal system within one of three fissure swarms in the Reykjanes Peninsula. It covers a large area and is commonly divided into subareas such as the Krísuvík field, the Trölladyngja field and the Sandfell field. A detailed alteration mapping was carried out by Vargas (1992) in the southeast part of the area between the Sveifluháls hyaloclastite ridge and the Geitahlíd-Kistufell mountains, and between lake Kleifarvatn and mountain Arnafell, which is presented in Figure 7.

The mapped area south of Kleifarvatn forms part of the Krísuvík fissure swarm, one of the main volcanotectonic units on the Reykjanes Peninsula. In Krísuvík, the surface rocks consist of a succession of Upper Pleistocene pillow lava basalts and hyaloclastites. In Postglacial time hydrothermal and phreatic explosion craters erupted, and welded lava and scoria cones were formed. Basaltic flows also reached down into the Krísuvík valley from eruption fissures of the Brennisteinsfjöll swarm in the northeast.

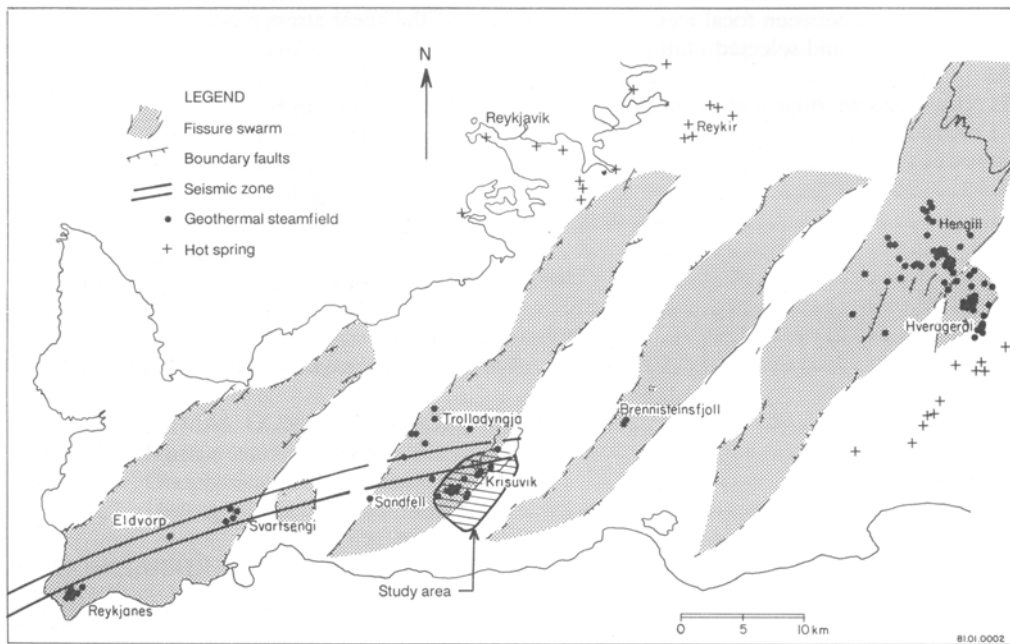


FIGURE 6: Location map of the Krísuvík area (after Saemundsson, 1980)

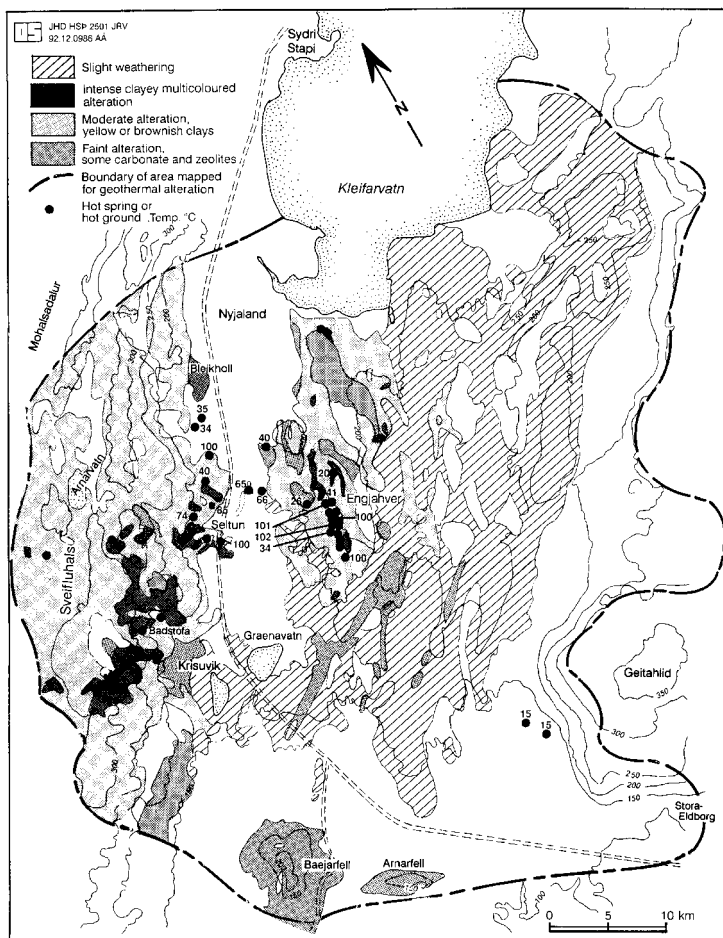


FIGURE 7: Alteration map of Krísuvík valley (Vargas, 1992)

The topography of the field is characterized by NE-SW trending hyaloclastite ridges in the west and a flat lying lava field with minor post-glacial volcanic edifices to the east (Malapitan, 1995). Surface geothermal manifestations consist of hot ground where bedrock has been altered at varying degrees by surficial acid leaching. It includes highly altered ground usually associated with steam vents and mud pools. Other thermal manifestations, including vein fillings, boiling springs, warm springs, hydrothermal explosion craters and mineralised waters are observed in the area (Figure 7). The groundwater table in the area is shallow.

The geothermal field, is characterized by a thick zone of convective thermal gradient, and wells show a thermal maximum in the top of this convective layer. According to Vargas, this is interpreted by assuming a hot lateral flow in the top of the geothermal system. The lateral flow would be related to the

vicinity of local upflow zones near wells showing the thermal reversal.

Wells drilled in the geothermal reservoir display lower temperatures at depth than expected. The mineral zonation usually indicates high temperature at shallow depths, even lacking the first zeolite zone, which is typical in the Icelandic geothermal fields. The zeolite zone was found at the surface in Baejarfell and Árnafell. The cooling of the geothermal reservoir has been ascribed to the occurrence of hydrothermal and phreatic explosions common in the area. The hydrothermal explosions would require boiling at shallow depth. This is compatible with the high-temperature mineralogy.

5.2 Schlumberger soundings (DC method)

Previous geophysical work. In Iceland, Schlumberger soundings have been used in regional reconnaissance surveys for low-temperature geothermal resources outside the volcanic zones and for mapping high-temperature geothermal systems in the volcanic zone. Resistivity profiling has mainly been used for locating vertical or near-vertical aquifers for low-temperature geothermal water and vertical resistivity boundaries in high-temperature geothermal systems (Árnasson, 1989).

A number of Schlumberger soundings data have been carried out in the area from Trölladyngja extending southwest to Sandfell and in the east between lake Kleifarvatn and Geitahlíð mountain. The survey included most of the area in Krísuvík valley shown on the alteration map (Figure 7). The data used were collected by geophysicists from Orkustofnun in 1986 and 1987. The locations and elevations of the Schlumberger soundings are presented in Appendix I (Table 1) (Kebede, 2001) and in Figure 8.

From the previous work, it has been argued that the bedrock resistivity at depth in the Krísuvík area is influenced by the relative position of the water table, water salinity, acid surface leaching (ground alteration) and underground temperature. High resistivity values are predominant at the surface in the Postglacial lava fields except in areas affected by surficial acid leaching (Marita, 1986; Kanganjua, 1987). Widespread low-resistivity layers (8 Ωm) in the uppermost 500 m correlate with geothermal activities in permeable near horizontal layers of hyaloclastite breccias; below which cooler and denser lavas dominate, manifested by increased resistivity with depth (10-80 Ωm). Inside the low resistivity area, several smaller areas of extra low resistivity (3-5 Ωm) were observed and interpreted as up-flow zones (Georgsson, 1987).

The main purpose of the present interpretation is to look for an additional understanding of the

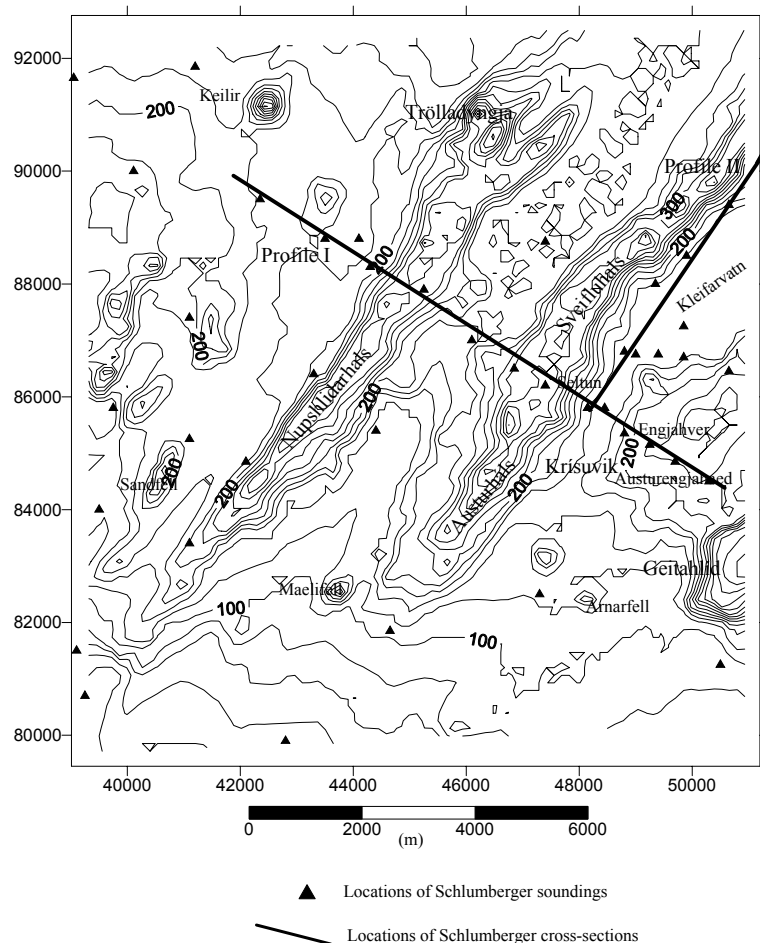


FIGURE 8: Location map of Schlumberger soundings

water- rock system related with the geothermal manifestations and structural conditions in the area. And as a part of the training programme, to make comparisons of the results with the results of a TEM survey made in the same area.

5.2.1 One-dimensional interpretation

The Schlumberger sounding curves were interpreted by one-dimensional inversion using the programme SLINV. The corresponding model curves are presented in Appendix II (Kebede, 2001). As can be seen there, most of the calculated curves fit the measured curves reasonably well with few exceptions like sounding TD074. Sounding TD074 and TD078 are on the same locations but the axis of the *AB* arms are N120°E and N30°E, respectively, and the difference in the resistivity curves may be due to different geological features encountered for the two orientations. The results of the interpretation of the Schlumberger data are presented here as iso-resistivity maps and two resistivity profiles, where the station arrangements allows profiles to be drawn with some confidence. The locations of the profiles is shown on Figure 8.

Iso-resistivity maps.

To study the subsurface resistivity distribution of the area, iso-resistivity maps at different elevations (relative to sea level) are presented. Zones of different resistivity values are grouped in terms of magnitude as high (>200 Ωm), moderately high (50-200 Ωm), moderately low (10-50 Ωm), low resistivities (5-10 Ωm), and very low resistivities (< 5 Ωm). In order to make a meaningful interpretation of conditions pertaining to the resistivity characteristics of the geothermal areas, high resistivity below low-resistivity formation is delineated and indicated with a special attribute in the iso-resistivity maps.

At 100 m a.s.l., most of the area is covered by high resistivity values except in the area near the Sveifluháls hyaloclastite ridge, Figure 9. The low-resistivity anomaly at this level is less than 10 Ωm in general and is only confined near Seltún, and high resistivity below low resistivity is observed between Seltún and Engjahver. At sea level, the resistivity is observed to be reduced from very high to a few hundreds of Ωm in most places (Figure 10). The low-resistivity anomaly and the high resistivity below low

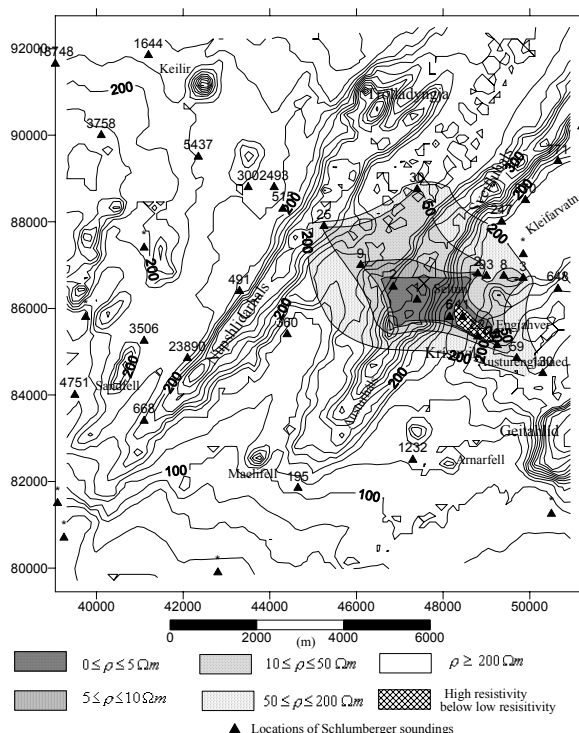


FIGURE 9: Resistivity contour map at 100 m a.s.l.

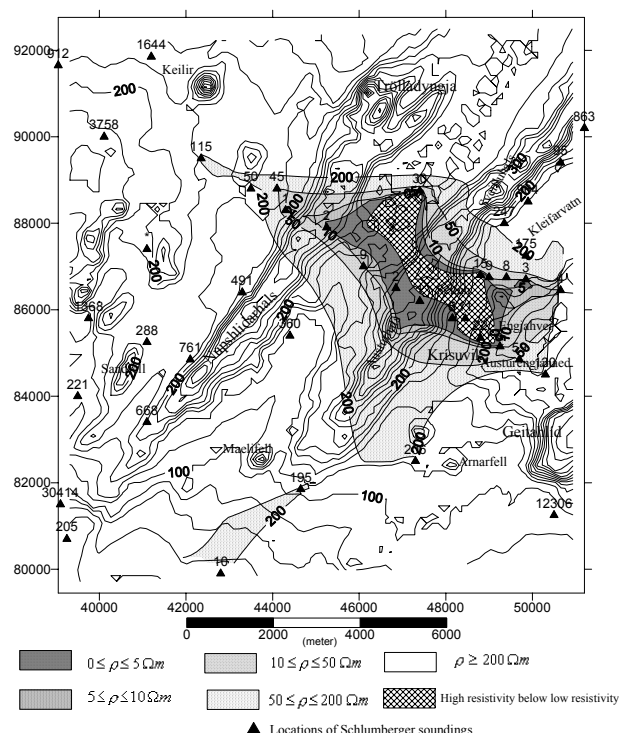


FIGURE 10: Resistivity contour map at sea level

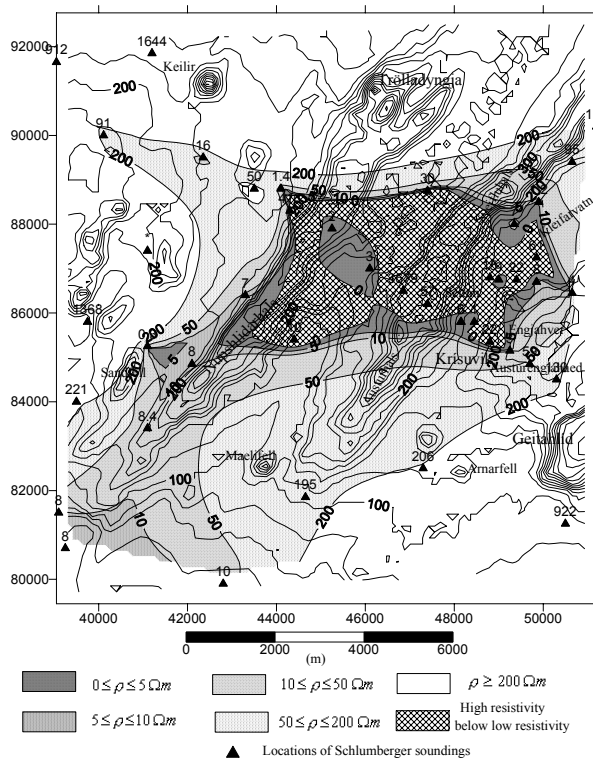


FIGURE 11: Resistivity contour map at 100 m b.s.l.

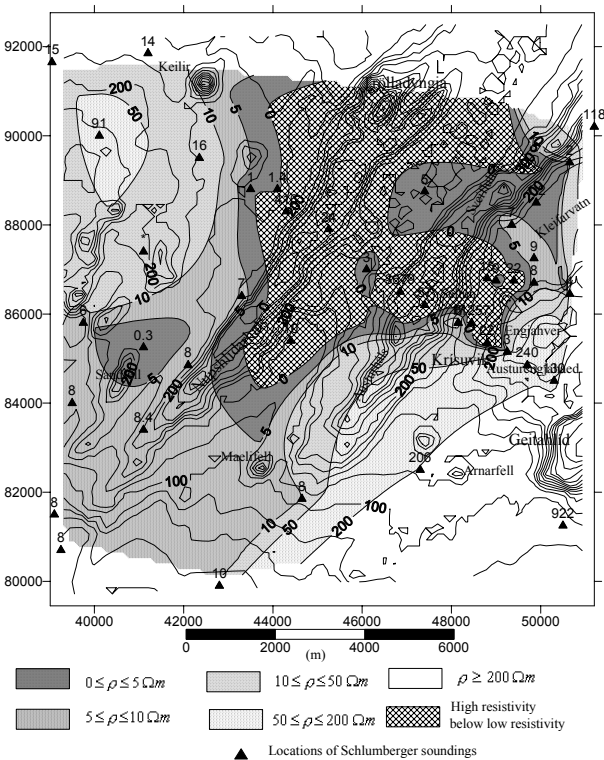


FIGURE 12: Resistivity contour map at 200 m b.s.l.

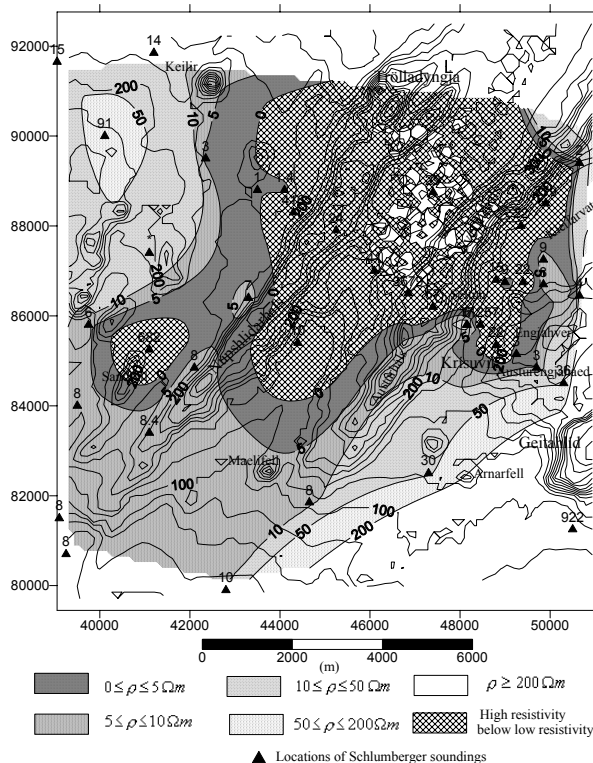


FIGURE 13: Resistivity contour map at 300 m b.s.l.

resistivity, observed at 100 m a.s.l., are now observed to extend to the western ridge (Núpslíðarháls). At greater depths (100 and 200 m b.s.l.) a significant reduction of the resistivity is observed in the southwest region (in the vicinity of Sandfell and Núpslíðarháls) and extends to the northeast covering most of the central area, as can be seen in Figures 11 and 12. This reduction in resistivity with further depth (300 m b.s.l.) is also revealed in Figure 13. The high resistivity below low resistivity is observed to cover most of the central and northeastern parts of the area beneath the two hyaloclastite ridges and in the southwest near Sandfell. The southeastern part of the area is, on the other hand, characterized by high resistivity, and moderate to low resistivity is observed in the remaining part of the area.

In order to have a clear picture of the resistivity structure with depth, two resistivity cross-sections across Profile I (PI) and Profile II (PII) were taken. The locations of the profiles are indicated in Figure 8.

Profile I is about 10 km long and it has an approximate orientation of N120°E. The profile crosses the two hyaloclastite ridges (Sveifluháls and Núpslíðarháls) and is nearly perpendicular to the direction of the general geological structure of the area, N40°E. The profile intercepts most of the geothermal manifestations mapped in Figure 7. The resistivity cross-section along this line is presented in Figure 14. As can be seen, most parts of the section

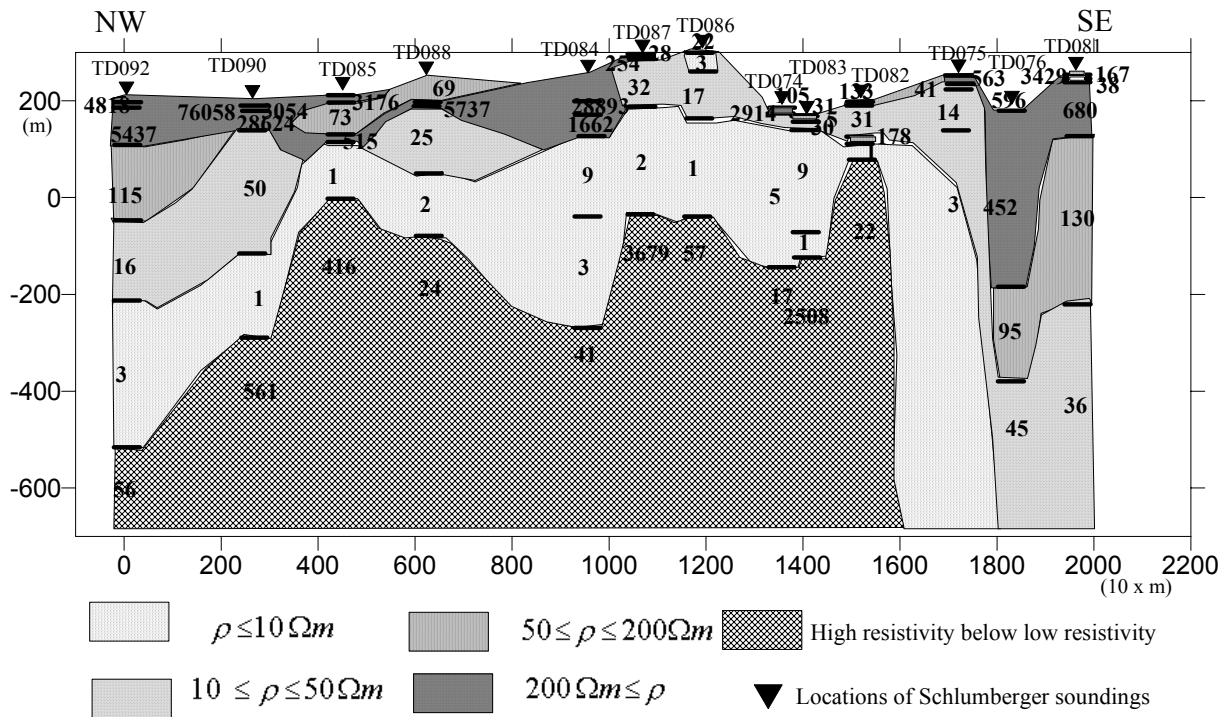


FIGURE 14: Resistivity cross-section across Profile I; note that the horizontal scale is multiplied by ten

are marked by a high-resistivity top layer ($> 200 \Omega m$) with thickness in the range of 100-200 m. Near TD088 and in the area between TD087 and TD075, the surface resistivity is marked by moderate resistivity values that are in the range of 10-15 Ωm .

Next to the high-resistivity surface layer, a resistivity structure with a reduced magnitude is observed. This layer has resistivity values in the range of 50-200 Ωm . The unit is observed near both ends of the cross-section. The third layer is a low-resistivity layer that extends from the northwest end of the profile (TD092) up to sounding TD075 in the southeast where it is bounded by a higher resistivity structure at the right flank of the section. This layer has a resistivity value less than 10 Ωm and different thicknesses from a few metres to about 300 m (beneath TD092). This low-resistivity layer trends out of the section in the northwestern part, but is observed to continue vertically to a greater depth beneath TD075 in the southeastern part.

The fourth layer is generally a high-resistivity structure beneath the low-resistivity layer just discussed. It consists of different high resistivity values between 15 Ωm and more than 1000 Ωm at depth but it should be noted that the actual resistivity values of this layer are often poorly defined in the inversion.

Profile II is located in the northeastern part of the survey area, between the Sveifluháls ridge and Lake Kleifarvatn. It intersects PI at sounding point TD074 near Seltún. It has an orientation of about N35°E, a length of about 5 km and its orientation is along the general trend of the fissure swarms in the area.

The resistivity cross-section of Profile II is presented in Figure 15. The resistivity structure along the Sveifluháls ridge is marked by a high-resistivity top layer having values $> 200 \Omega m$ and thickness in the range 100-150 m in most parts of the line. The anomaly thins out towards TD097 where it is succeeded by a thin, medium-resistivity unit ($\leq 200 \Omega m$) near sounding points TD078 and TD096. This medium-resistivity structure is also observed to extend towards TD094 beneath the high-resistivity top layer, getting thicker in dimension. Below this resistivity, a continuous low resistivity is underlain by high-resistivity structure at bottom.

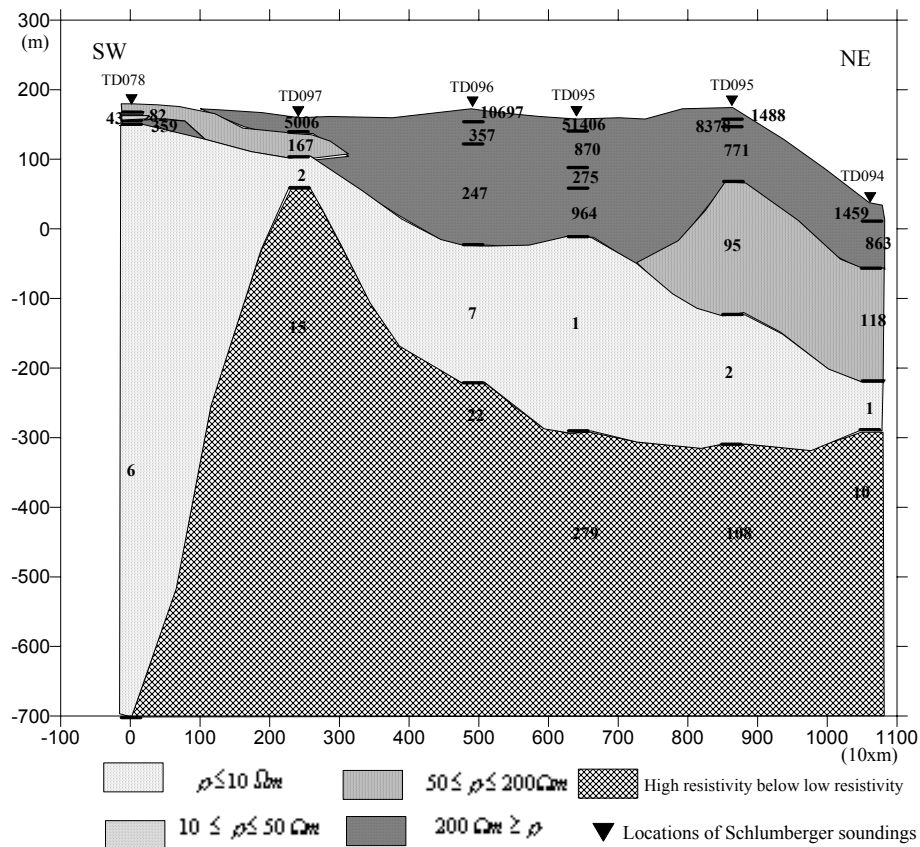


FIGURE 15: Resistivity cross-section across Profile II; note that the horizontal scale is multiplied by ten

5.2.2 Results

In general, the geothermal reservoir rocks are characterized by low-resistivity anomalies. From case histories of the Icelandic high-temperature geothermal fields, Nesjavellir, Hengill, and Krafla, the presence of high resistivity beneath low-resistivity formations is reported. The observed resistivity structure was found to correlate with hydrothermal alteration minerals. In the present study, such an anomalous zone is also delineated and mapped as can be seen in Figures 14 and 15.

The high surface resistivity observed over both sections most likely represents fresh basaltic rocks of post-glacial volcanism. In the areas where the surface resistivity is in the range of 10-50 Ωm , as between TD086 and TD087 (near Seltún), surface geothermal manifestations with moderate alteration (yellow or brownish clay) and mud pools are observed. Similarly, near TD075 there is a big fumarole next to Austurengjahver, and in the areas near Engjahver hot springs, hot ground and altered rocks are also observed. Mud pools and steam vents occur near soundings TD074 (TD078) and TD083 (Malapitan, 1995).

The low resistivity anomaly in Profile I indicates that the low-temperature alteration minerals, smectite and zeolite come into play. This zone extends from northwest of Profile I and continues to the southeast part of the profile, where it is bounded by a highly resistive block between TD075 and TD076. It appears as a vertical low-resistivity structure that extends from a few tens of metres from the surface to a greater depth at this location. A similar resistivity layering is observed in Profile II as in Profile I. Both sections show a typical resistivity structure of a high-temperature geothermal system with a low-resistivity cap underlain by a more resistive core that marks the zone of high-temperature alteration minerals, the chlorite zone.

Interpretation of the resistivity structure of the Krísuvík geothermal field is made by comparing the observed anomalous zones with the available geological information and the alteration map shown in Figures 7. The following conclusions are drawn:

- The near surface high-resistivity layer, $\geq 200 \Omega\text{m}$, is interpreted as fresh basaltic rock of postglacial volcanism.
- The next layer, $50\text{-}200 \Omega\text{m}$, may show the response of basaltic rock that is affected by the ground water and slight alteration. It is mostly seen beneath the high resistivity surface rocks.
- Moderate resistivity values $10\text{-}50 \Omega\text{m}$ are related to moderately hydrothermally altered rocks. These resistivity values are observed at the surface where the area is affected by hydrothermal alteration and other geothermal manifestations are present.
- The resistivity values lower than $10 \Omega\text{m}$ are taken as a low-resistivity layer reflecting highly altered rocks in the smectite-zeolite zone, with temperature in the range of $50\text{-}200^\circ\text{C}$. The extent of this formation is about 8 km, starting from TD075 to the northwest in Profile I, and is seen along the whole of Profile II. The low-resistivity area in the iso-resistivity maps (Figures 12 and 13) trending in a SW-NE direction, reflects the top of the geothermal reservoir.
- The high resistivities below low resistivity in the central (beneath the two hyaloclastite ridges) and southwestern parts (near Sandfell) of the geothermal area are related to high-temperature ($T > 240^\circ\text{C}$) geothermal activity in the chlorite alteration zone. This is supported by surface geothermal manifestations. The high resistivity at depth in the southeast reflects cold basaltic rocks in the area.

5.3 TEM-Soundings

5.3.1 One-dimensional interpretation

Discussion of the theoretical aspects of the one-dimensional inversion program of TEM data (TINV) are given in Section 4.4. Eighty-three TEM soundings have been made in the same area that was covered by the Schlumberger survey, since 1986. For the present work only 53 soundings, fairly distributed in the area, were selected and interpreted by the author. The sounding coordinates are given in Appendix I, Table 2 (Kebede, 2001) and the locations are shown in Figure 16. The one-dimensional models obtained after using the inversion program are presented in Appendix III (Kebede, 2001). For comparison purposes of the two methods, an iso-resistivity map at 300 m b.s.l., was made Figure 17, and a TEM cross-section (Profile), in the central part

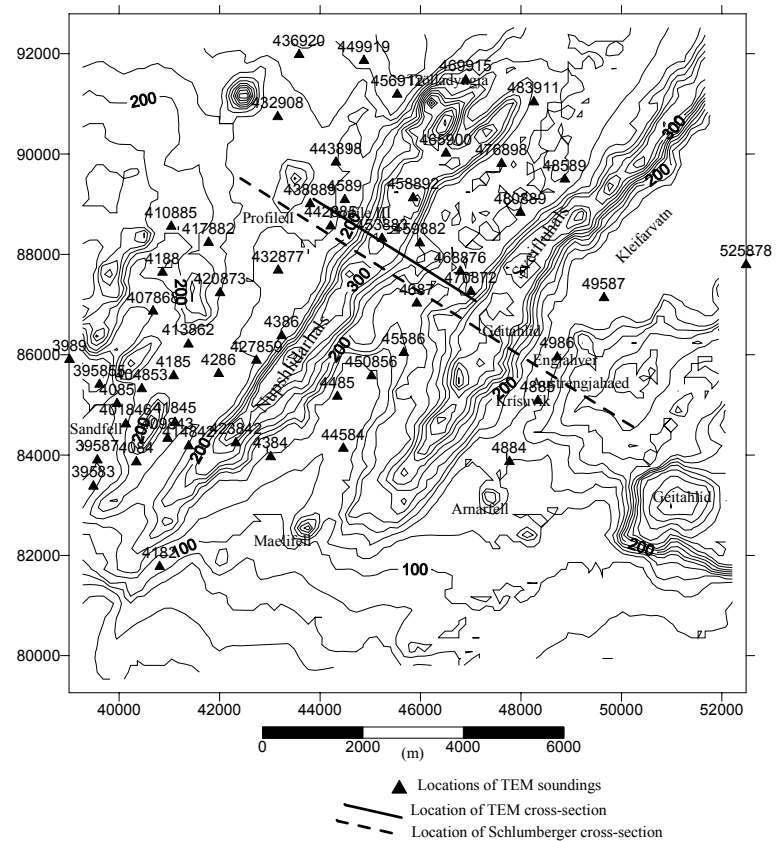


FIGURE 16: Locations of TEM soundings and cross-section

of the survey area, parallel to PII, was made and is presented in Figure 18. A new TEM sounding (525878) at coordinates (52483, 87790) in the southeastern part of Lake Kleifarvatn, was made for the purpose of demonstrating data acquisition of the TEM survey.

5.3.2 Results

Iso-resistivity map. The main characters of the resistivity distribution, as observed by the Schlumberger survey at a comparable depth level, 300 m b.s.l., is also observed in the iso-resistivity map based on the TEM soundings (Figure 17). As can be seen from the figure, high-resistivity below a low-resistivity layer is open to the northeast and extends towards Lake Kleifarvatn and in the direction of Engjahver. In the south end of lake Kleifarvatn, new geothermal manifestations are exposed at the surface due to subsidence of the water level of the lake. These manifestations and those mapped in the alteration map, Figure 7, show that the anomaly pattern reveals a high-temperature geothermal system in the area.

Profile III. A TEM cross-section along Profile III is made using the data found in the vicinity of PI across the ridge Núpshlíðarháls. The data points are projected onto the profile giving an approximate length of 3.6 km. It has a similar orientation to that of Profile I. Profile III reveals similar resistivity structures as the corresponding portion of the Schlumberger profile, as can be seen by comparing Figures 14 and 18. A close inspection of the sections reveals that in the Schlumberger soundings, resolve near-surface high-resistivity variations which in the TEM results appear as more lumped units.

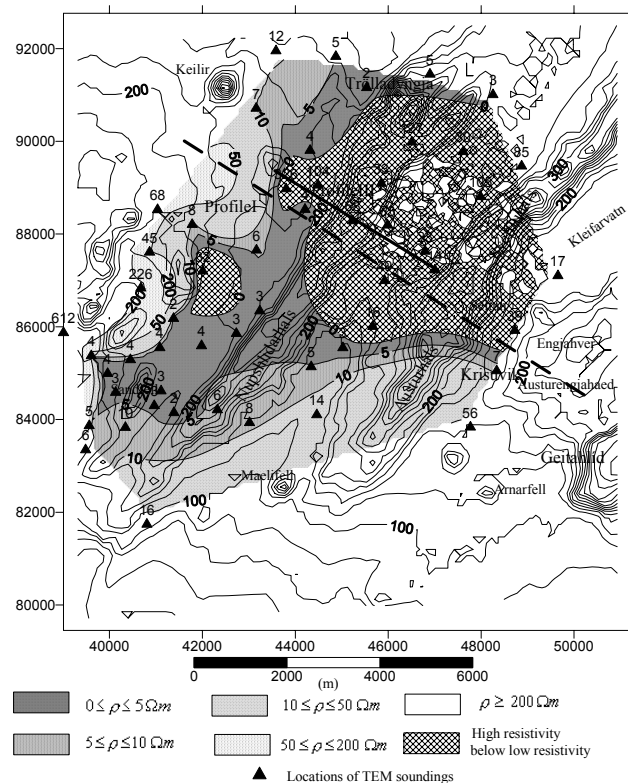


FIGURE 17: Resistivity contour map, at 300 m b.s.l.

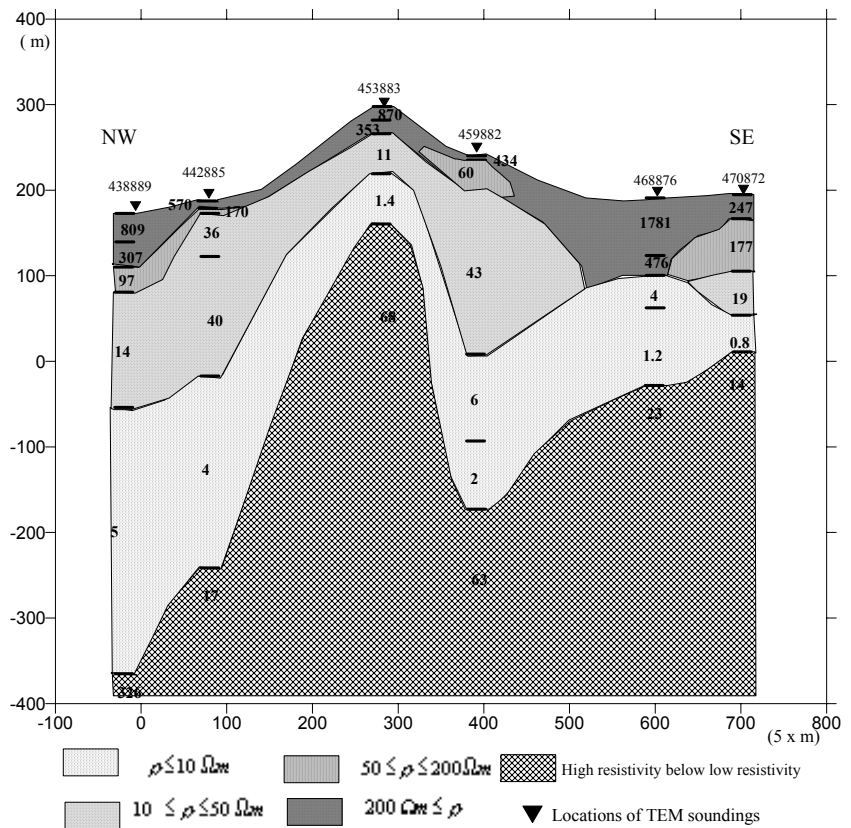


FIGURE 18: Resistivity cross-section across Profile III, note that the horizontal scale is multiplied by five

Sounding 525878 is not included in the data set used for the iso-resistivity map because it is a bit far from other TEM-soundings but its location is shown on the location map for the TEM survey (Figure 16). Nevertheless, the sounding adds valuable information to the TEM data southwest of the lake. As can be seen from the curve (Figure 19), a decrease in the resistivity with depth characterizes the sounding. The absence of the high-resistivity bottom layer in the model indicates that the resistive inner core of the high-temperature reservoir in the southwestern part of the lake does not extend towards this sounding point.

6. COMPARISON OF SCHLUMBERGER AND TEM RESULTS

Generally the Schlumberger and TEM data gathered in the Krísuvík geothermal field show similar resistivity structure. Detailed comparison of the maps reveals slight discrepancies. These discrepancies are reflected in the delineation of the low-resistivity zones in the iso-resistivity maps (Figures 13 and 17), and in the resolution of the high-resistivity layers close to the surface (uppermost 100 m) in the cross-sections (Figures 14 and 18). In TEM, the low-resistivity values at depth are significantly lower than the values in the Schlumberger map indicating that low-resistivity anomalies at depth are better resolved by the TEM method. Similar comparison of the cross-sections, profiles I and III reveals that high resistivities in the uppermost layer, in the upper 100 m, are better resolved in the Schlumberger survey. The TEM results lack this detail in the uppermost layers, which is due to the limitation of the equipment to sample the transients at very early times.

Two Schlumberger sounding curves at the same location, TD074 and TD078, along with a neighbouring TEM-sounding (4986) are compared in Figure 20. Sounding TD074 has an electrode configuration that is approximately perpendicular to the general strike direction of the fissure swarms whereas TD078 is nearly parallel to it (refer to Table 1 and Table 2 in Appendix I). The two Schlumberger curves are quite different from each other both in values and shape but the TEM gives a well-defined curve.

The advantages and disadvantages of the central-loop TEM over the Schlumberger (DC) method are summarized as follows (Árnason, 1989):

- In a central-loop TEM survey the transmitter couples inductively to the earth and no current has to be injected into the ground. This makes the method easily applicable in areas where the surface is dry and resistive, where Schlumberger soundings can be difficult.
- The monitored signal at the surface is a decaying magnetic field but not the electric field. This makes the TEM measurement much less dependent on local resistivity conditions at the receiver site. Distortion due to local resistivity inhomogeneities at the receiver site can be a severe problem in DC-soundings.
- The TEM method is less sensitive to lateral resistivity variations as compared to DC.
- DC-sounding the monitored signal is low when subsurface resistivity is low, as in geothermal areas, whereas in TEM soundings the situation is the reverse, the lower the resistivity the stronger the signal.

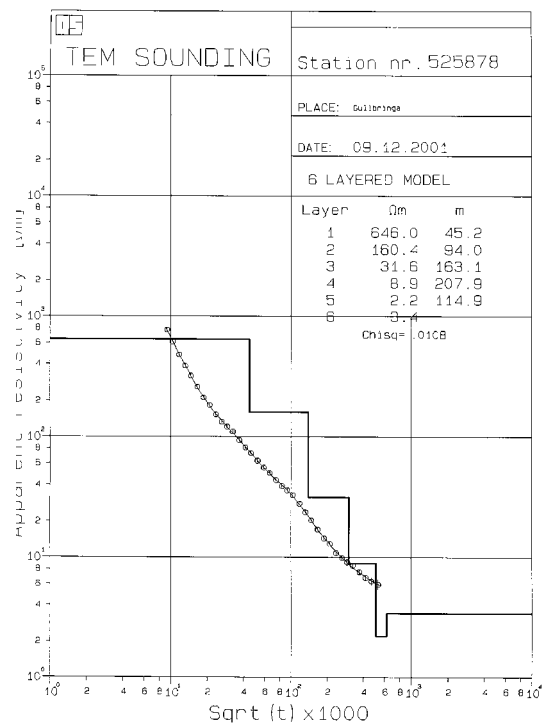
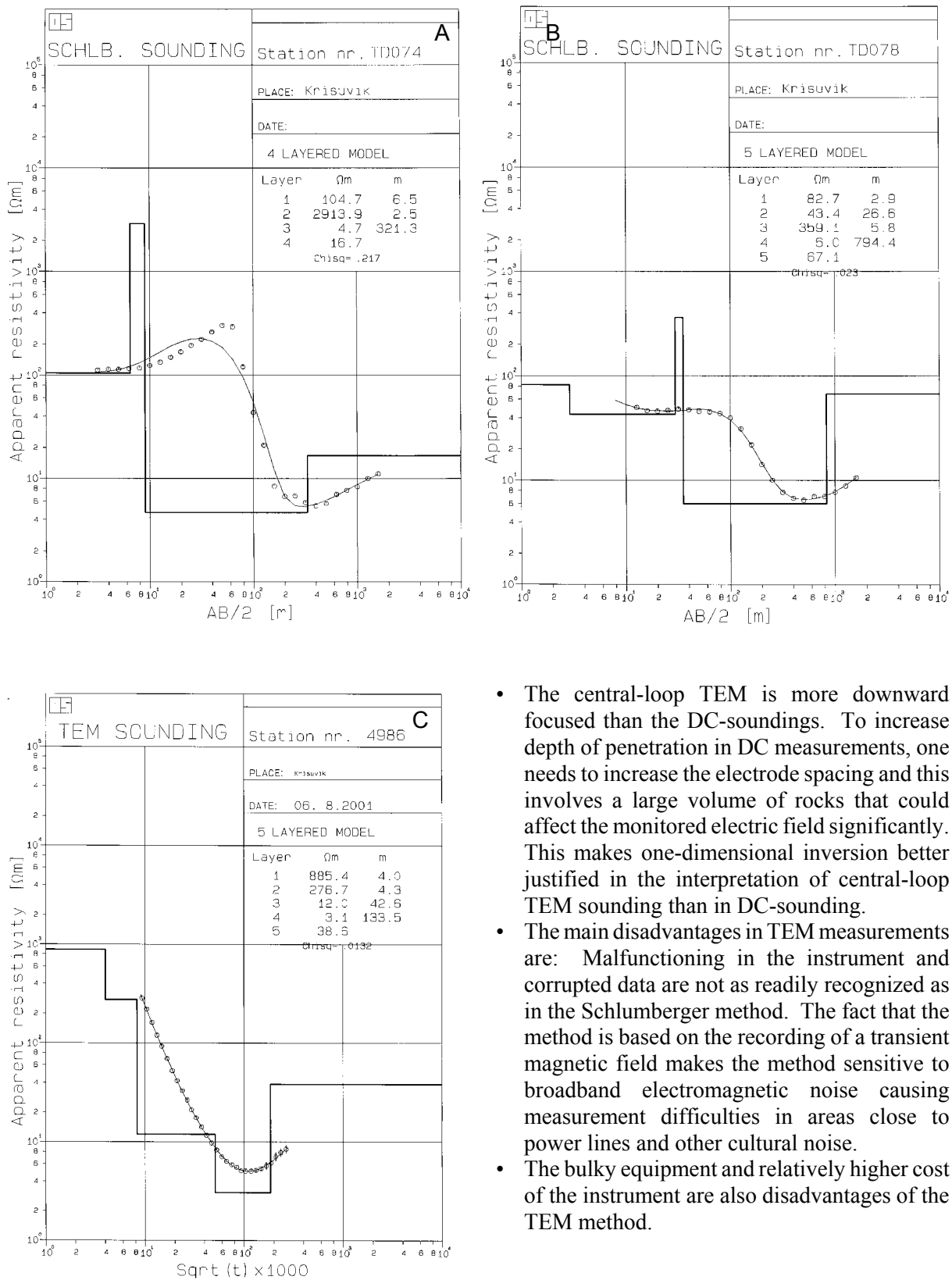


FIGURE 19: TEM sounding 525878 in Krísuvík area and its one-dimensional interpretation



- The central-loop TEM is more downward focused than the DC-soundings. To increase depth of penetration in DC measurements, one needs to increase the electrode spacing and this involves a large volume of rocks that could affect the monitored electric field significantly. This makes one-dimensional inversion better justified in the interpretation of central-loop TEM sounding than in DC-sounding.
- The main disadvantages in TEM measurements are: Malfunctioning in the instrument and corrupted data are not as readily recognized as in the Schlumberger method. The fact that the method is based on the recording of a transient magnetic field makes the method sensitive to broadband electromagnetic noise causing measurement difficulties in areas close to power lines and other cultural noise.
- The bulky equipment and relatively higher cost of the instrument are also disadvantages of the TEM method.

FIGURE 22: Comparison of one-dimensional interpretation of Schlumberger soundings
 a) TD074 and b) TD078, and
 c) TEM sounding 4986

7. GENERAL CONCLUSIONS

In the study of the Krísuvík area, 43 Schlumberger and 52 central-loop TEM soundings are interpreted using one-dimensional inversion programs SLINV and TINV, respectively. The data are presented as iso-resistivity maps and resistivity cross-sections using both data sets and the results are discussed and compared. For the purpose of training, one TEM sounding was made southeast of lake Kleifarvatn.

The DC and TEM methods mapped the resistivity structure of the Krísuvík area showing good correlation with the available geological information. According to the result of the two methods the Krísuvík geothermal area is characterized by a high-resistivity surface layer ($>200 \Omega\text{m}$), which is interpreted as cold fresh lava rocks in the area. Reduction of resistivity values with depth is noticed. This reduction in resistivity with depth can be explained by low-grade alteration below the ground water level or it may be related to hyaloclastite rock formations in the subsurface. Moderately hydrothermally altered rocks in the area are characterized by moderate resistivity values ($\leq 50 \Omega\text{m}$) which are observed to coincide with surface geothermal manifestations in the northeast part of the study area.

Two possible zones of high-temperature geothermal reservoirs are delineated, one near Sandfell and the other in the northeastern part of the study area. The latter is open to the north and northeast, beneath the lake. The typical resistivity structure of high-temperature geothermal fields seen elsewhere in Iceland, characterized by a low-resistivity cap underlain by a resistive core, is also found in the Krísuvík system

The sounding curve 525878 at (52483,87790) shows a decrease in resistivity with depth indicating that the observed anomaly southwest of lake Kleifarvatn has an eastern boundary under the lake. From comparisons of the results of the DC and TEM methods and from the experience obtained in resistivity measurements of high-temperature geothermal fields of Iceland, the central-loop TEM method is found to be more effective in resistivity mapping in dry and resistive ground conditions. The response is mainly affected by geological conditions beneath the sounding point and, thus, TEM has a better anomaly resolution at depth than Schlumberger soundings.

ACKNOWLEDGEMENTS

I would like to convey my deepest gratitude to Dr. Ingvar Fridleifsson, director of the United Nations University Geothermal Training Programme and to Mr. Lúdvík S. Georgsson, deputy director of UNU for accepting me as a UNU fellow of the year 2001 and to Gudrún Bjarnadóttir for the assistance she provided me during my stay in Iceland. I would like to extend my best thanks to my advisor Dr. Knútur Árnason for the lectures he gave me and for sharing his long experience in geophysical exploration and for the dedication in his critical comments on my project. Also I would like to convey my thanks to all the lecturers that participated in the six-month course and to staff members of geophysics, Dr. Hjálmar Eysteinnsson, Karl Gunnarsson and Ragna Karlsdóttir for the lectures and assistance they provided me during my study. I extend special thanks to the Geological Survey of Ethiopia for allowing me to participate in this programme.

REFERENCES

- Archie, G.E., 1942: The electrical resistivity log as an aid in determining some reservoir characteristics. *Tran. AIME*, 146, 54-67.
- Árnason, K., 1984: The effect of finite electrode separation on Schlumberger soundings. *54th Annual International SEG Meeting, Atlanta, Expanded Abstracts*, 129-132.
- Árnason, K., 1989: *Central loop transient electromagnetic sounding over a horizontally layered earth*. Orkustofnun, Reykjavík, report OS-89032/JHD-06, 129 pp.
- Árnason, K., and Hersir, G.P., 1988: *One-dimensional inversion of Schlumberger resistivity soundings. Computer program description and user's guide*. UNU G.T.P., Iceland, report 8, 59 pp.
- Árnason, K., Karlsdóttir, R., Eysteinnsson, H., Flóvenz, Ó.G., and Gudlaugsson, S.Th., 2000: The resistivity structure of high-temperature geothermal systems in Iceland. *Proceedings of the World Geothermal Congress 2000, Kyushu-Tohoku, Japan*, 923-928.
- Björnsson, A., 1980: Geophysical methods used in geothermal exploration (in Icelandic with English summary). *Náttúrufræðingurinn*, 50, no. 3-4, 227-249.
- Dakhnov, V.N., 1962: Geophysical well logging. *Q. Colorado Sch. Mines*, 57-2, 445 pp.
- Flóvenz, Ó.G., Georgsson, L.S., and Árnason, K., 1985: Resistivity structure of the upper crust in Iceland, *J. Geophys. Res.*, 90-B12, 10,136-10,150.
- Fridleifsson, I.B., 1979: Geothermal activity in Iceland. *Jökull*, 29, 47-56.
- Georgsson, L.S., 1987: Application of resistivity sounding in the exploration of high-temperature geothermal areas in Iceland with examples from the Trölladyngja-Krýsuvík area, SW-Iceland. *Technical Programme and Abstracts of Exploration '87, Toronto*, 52.
- Hersir G.P. and Björnsson A., 1991: *Geophysical exploration for geothermal resources. Principles and applications*. UNU G.T.P., Iceland, report 15, 94 pp.
- Kanyanjua, A.W., 1987: *Schlumberger vertical sounding techniques and interpretations: Krýsuvík, Iceland and Menengai, Kenya*. UNU G.T.P., Iceland, report 12, 55 pp.
- Kebede, Y., 2001: Appendices to the report: Application of the resistivity method in the Krýsuvík geothermal area, Reykjanes Peninsula, SW-Iceland. UNU, G.T.P., Iceland, report 6 appendices, 29 pp.
- Keller, G.V., and Frischknecht, F.C., 1966: *Electrical methods in geophysical prospecting*. Pergamon Press Ltd., Oxford, 527 pp.
- Koefoed, O., 1979: *Geosounding principles, I: Resistivity sounding measurements*. Elsevier Scientific Publishing Co., Amsterdam, 276 pp.
- Malapitan, R.T., 1995: Borehole geology and hydrothermal alteration of well KR-9, Krýsuvík, SW-Iceland. Report 8 in: *Geothermal Training in Iceland 1995*. UNU G.T.P., Iceland, 185-206.
- Mariita, N.O., 1986: *Schlumberger vertical soundings: Techniques and interpretations with examples from Krýsuvík and Glerárdalur, Iceland and Olkaria, Kenya*. UNU G.T.P., Iceland, report 5, 48 pp.

Quist, A.S., and Marshall, W.L., 1968: Electrical conductances of aqueous sodium chloride solutions from 0 to 800°C and at pressures to 4000 bars. *J. Phys. Chem.*, 72, 684-703.

Saemundsson, K., 1979: Outline of the geology of Iceland. *Jökull* 29, 7-28.

Saemundsson, K., 1980: Application of geology in geothermal research in Iceland (in Icelandic with English summary). *Náttúrufræðingurinn*, 50, no. 3-4, 157-188.

Stefánsson, V., Axelsson, G., and Sigurdsson, Ó., 1982: Resistivity logging of fractured basalt. *Proceedings of the 8th Workshop on Geothermal Reservoir Engineering, Stanford University, Ca*, 189-195.

Vargas M., J.R., 1992: *Geology and geothermal considerations of Krisuvik valley, Reykjanes, Iceland*. UNU G.T.P., Iceland, report 13, 35 pp.

Zohdy, A.A.R., 1980: Electrical methods. In: *Application of surface geophysics to ground-water investigations*. U.S. Geological Survey, Arlington, report, 5-66.